NASA TECHNICAL NOTE

NASA TN D-8386

EFFECTS OF GEOMETRY AND JET VELOCITY ON NOISE ASSOCIATED WITH AN UPPER-SURFACE-BLOWING MODEL

Lorenzo R. Clark and James C. Yu

Langley Research Center
Hampton, Va. 23665

NATIONAL AERONAUTICS AND SPACE ADMINISTRATION • WASHINGTON, D. C. • MARCH 1977

7/13/77 DM

ERRATA

NASA Technical Note D-8386

EFFECTS OF GEOMETRY AND JET VELOCITY ON NOISE ASSOCIATED WITH AN UPPER-SURFACE-BLOWING MODEL

Lorenzo R. Clark and James C. Yu
March 1977

Page 26: The vertical scales in figures 10(a) and 10(b) are incorrect and the predicted value of OASPL in figure 10(b) is in error. Replace page 26 with the attached corrected page 26.

Issued June 1977

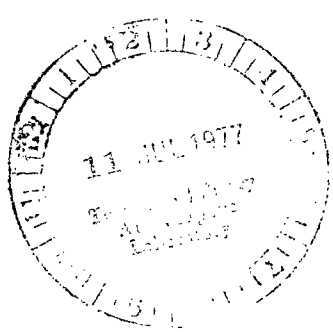

1. Report No.	2. Government Accession No.	3. Recipient's Catalog No.
NASA TN D-8386		

4. Title and Subtitle
EFFECTS OF GEOMETRY AND JET VELOCITY ON NOISE ASSOCIATED WITH AN UPPER-SURFACE-BLOWING MODEL

5. Report Date
March 1977

6. Performing Organization Code

7. Author(s)
Lorenzo R. Clark and James C. Yu

8. Performing Organization Report No.
L-11147

10. Work Unit No.
505-03-11-04

9. Performing Organization Name and Address
NASA Langley Research Center
Hampton, VA 23665

11. Contract or Grant No.

13. Type of Report and Period Covered
Technical Note

12. Sponsoring Agency Name and Address
National Aeronautics and Space Administration
Washington, DC 20546

14. Sponsoring Agency Code

15. Supplementary Notes
Lorenzo R. Clark: Langley Research Center.
James C. Yu: Joint Institute for Advancement of Flight Sciences, George Washington University.

16. Abstract

An investigation of the noise characteristics associated with various upper-surface-blowing configurations has been performed with a small model. The model consisted of a plate and flap assembly (simulated wing with flap) attached to a rectangular nozzle. Nozzle aspect ratio, flow-run length, and flap-deflection angle are the main experimental parameters investigated in this study. Three nozzle-exit velocities were used.

The normalized noise spectra obtained for different nozzle aspect ratios proved to be similar in terms of Strouhal number based on jet velocity and flow-run length. Consequently, the need for knowing local flow velocity and length scales (for example, at the flap trailing edge) as required in some of the existing noise prediction schemes is eliminated. The present data are compared with results computed from three different noise prediction schemes, and the validity of each scheme is assessed. A simple method is also proposed to evaluate the frequency dependence of acoustic shielding obtained with the simulated wing flap.

17. Key Words (Suggested by Author(s))	18. Distribution Statement
Rectangular nozzle Upper-surface blowing Data similarity Acoustic shielding	Unclassified - Unlimited Subject Category 71

19. Security Classif. (of this report)	20. Security Classif. (of this page)	21. No. of Pages	22. Price*
Unclassified	Unclassified	32	$4.00

* For sale by the National Technical Information Service, Springfield, Virginia 22161

EFFECTS OF GEOMETRY AND JET VELOCITY ON NOISE ASSOCIATED WITH AN UPPER-SURFACE-BLOWING MODEL

Lorenzo R. Clark and James C. Yu*
Langley Research Center

SUMMARY

A parametric study has been made of the sound field generated by jet flow which emanates from slot nozzles and passes over the upper surface of a simulated wing and flap. The acoustic data obtained were found to be similar when plotted against a Strouhal number based on jet velocity and flow-run length. Based on this finding, a simple method was derived to evaluate acoustic shielding quantitatively. The method yields a mean curve which appears to be valid for model data. However, a noticeable discrepancy occurs when the mean curve is compared with data obtained with a large simulated short takeoff and landing (STOL) aircraft. This discrepancy is attributable primarily to high frequency turbofan engine aft-end noise. The acoustic shielding indicated in the various data comparisons was found to increase with increasing Strouhal number.

Data from the present study were also compared with various prediction schemes in the literature. The extent to which the measured and predicted data agreed seemed to depend upon the particular prediction scheme chosen.

INTRODUCTION

Maintenance of low noise levels over communities near airports is one of the most important requirements for public acceptance of new commercial aircraft. Low noise levels are vital for the short takeoff and landing (STOL) short haul system of air transportation currently under consideration for alleviation of transportation congestion. Upper-surface-blowing (engine-over-the-wing) systems have shown considerable promise in meeting these low noise requirements in comparison with other powered-lift concepts. One of the advantages attributed to upper-surface-blowing configurations is the possible benefit of acoustic shielding that could result from the presence of a wing flap between the source and an observer. The extent of noise suppression obtainable with this arrangement is a function of such parameters as nozzle aspect ratio, flow-run length, and flap-deflection angle.

Several experimental studies have been made with small-scale models (see refs. 1 and 2, 5 to 9, and 11 to 20), and various sound generating mechanisms have been identified. In addition to the preponderance of small-scale data available in the literature, recent acoustic results from static and simulated

*Joint Institute for Advancement of Flight Sciences, George Washington University.

low forward-speed tests of a large-scale model of an aircraft configuration have been presented in reference 20. In addition, a few documents such as references 3 and 4, 10, 12, and 21 to 23 have reported primarily theoretical investigations of the noise field associated with flows interacting with surfaces.

In order to predict the noise generated by an upper-surface-blowing configuration, spectral similarity of the radiated noise as well as the overall noise level should be established in terms of physical variables related to the flow. Past research studies have established that the overall noise is proportional to the nozzle-exit velocity raised to a power between 5 and 6. Reference 3, for instance, has also presented spectral data that were similar for an upper-surface-blowing model that consisted of a nozzle-plate arrangement, but the similarity of data was based on flow velocity and flow scale local to the trailing edge of the flap. Such velocity and scale may, however, be difficult to compute for arbitrary nozzle-plate configurations. Consequently, computation would be simplified if the spectral similarity of these configurations could be based on the operating conditions of the nozzle and on the physical length of the wing flap. An attempt to do this calculation for a small model is included in the present study. In addition, the data gathered in this study are used to test various noise prediction schemes in the existing literature.

Very few attempts have been made to quantify the effect of acoustic shielding. Therefore, a simple scheme for quantifying the shielding effect is proposed in this study. This scheme resulted from analyses of the present data and from comparisons made with other experimental data in the open literature.

SYMBOLS

c_f	flap chord, m
c_o	ambient speed of sound, m/sec
$D(\gamma)$	theoretical directivity as function of γ
f	one-third-octave band center frequency, Hz
f_p	peak one-third-octave band center frequency, Hz
h	height of rectangular-nozzle exit, m
ℓ	flow-run length along upper surface of plate between nozzle exit and flap trailing edge, m
M_j	jet Mach number referred to ambient speed of sound, V_j/c_o
OASPL	overall sound pressure level, dB
r	distance of microphone from nozzle exit, m
S	nondimensional frequency parameter, $f\ell/V_j$

SPL	sound pressure level, dB
V_j	nozzle-exit velocity, m/sec
V_m	maximum local velocity, m/sec
w	width of rectangular-nozzle exit, m
γ	angle measured from nozzle axis in plane perpendicular to wing flap (see fig. 4), deg
δ	deflection of flap measured from trailing edge of upper surface to wing-chord plane (see fig. 1), deg
δ'	distance between flap surface and maximum velocity location at flap trailing edge, m

MODEL AND TEST PROCEDURE

Test Model

A diagram of the model used in this study is shown in figure 1. This figure also shows the various nozzle-plate parameters investigated in this study. Each model configuration consisted of a plate attached to the flat side of the nozzle plenum chamber as shown by the photograph in figure 2. The dimensions of the nozzle-plate hardware are given in figure 3.

The model was tested with two nozzles having different aspect ratios w/h. In each case, however, the exit area was equivalent to the exit area of a circular nozzle 5.08 cm in diameter. The nozzle-exit geometry was changed by installing and tightly sealing a contoured insert inside the open end of the nozzle plenum chamber. An aluminum honeycomb section was inserted in the plenum chamber in an attempt to damp out the turbulence upstream of the nozzle exit.

Attached to the plate was a removable flap section with a fixed deflection angle δ. Flaps with deflection angles of 0°, 30°, and 60° were used during the tests. The chord c_f of these flaps was fixed at 0.061 m. However, the 30° and 60° flaps had 12.1 cm and 6.4 cm turning radii, respectively. The plate could be translated along the side of the plenum chamber; thereby, variation of flow-run length ℓ (the portion of the plate lying between the nozzle exit and flap trailing edge) was accomplished.

Table I gives the matrix of w/h (aspect ratio) and ℓ/h (ratio of flow-run length to nozzle height) values investigated in this study. The ranges of flap-deflection angle δ and jet velocity V_j tested are also given in table I.

Instrumentation

The noise measuring instrumentation consisted of four 0.64-cm-diameter free-field response condenser microphones mounted on a stationary boom. The micro-

phones were located in the plane perpendicular to the model plate, and the plane passed through the nozzle center line. Each system frequency response was flat to within $\pm$1.5 decibels (dB) from 50 Hz to 80 kHz. During the tests, the signals from the microphones were analyzed online by a real-time analyzer to obtain sound-pressure-level spectra graphs. All the readout equipment used to obtain data at the test site were housed in a nearby instrumentation van.

Test Setup

A photograph and diagram of the test setup are shown in figures 4(a) and 4(b), respectively. The model was mounted on top of an outdoor blowdown tank which served as a settling chamber. The blowdown technique used was considered necessary to eliminate the possibility of acoustic contamination by upstream valve noise. Cold compressed air was supplied to the chamber by opening a valve located near adjacent air storage tanks. The inner walls of the settling chamber were acoustically treated with 2.5-cm-thick acoustic foam material to attenuate standing wave patterns inside the tank. Figure 4(a) shows the four microphones used for obtaining noise measurements in the far field. As shown, microphones were located in the vertical plane at $\gamma = 40^{\circ}$, 70°, 90°, and 270°. The photograph in figure 4(a) also shows that each microphone was equipped with a windscreen for minimizing wind noise. The average overall background noise level during the tests was 68 $\pm$ 3 dB. The background noise was concentrated mainly at very low frequencies. Corrections for background noise were not made because of the large signal-to-noise ratio (typically 20 dB).

Test Procedure

Each model configuration was tested for conditions corresponding to zero forward velocity. All tests were conducted at nozzle pressure ratios of 1.2, 1.35, and 1.5, with corresponding nozzle-exit velocities of 174, 221, and 253 m/sec, respectively. Typical values of ambient temperature, barometric pressure, and relative humidity recorded during the data collection period were 23° C, 0.102 MPa, and 62 percent, respectively. No tests were conducted on days when the wind velocity exceeded 2.57 m/sec (or 5 knots). Neither were corrections made to the acoustic data to account for possible atmospheric effects.

For each model configuration tested, far-field acoustic measurements were made with each microphone. Each sound measurement system was calibrated at the beginning and end of each test day by use of an acoustic calibrator. The major emphasis in this report is placed on data obtained at $\gamma = 90^{\circ}$, a point which corresponds to a position directly beneath an aircraft.

The experimental operations were carried out by first pressurizing the settling chamber to 70 kPa. This pressurization was accomplished by sealing the nozzle with a plug that could be clamped over the nozzle exit and then released from a remote position. When the plug was released, it was forced clear of the nozzle as air exhausted from the exit. During this process, the settling chamber pressure was monitored with a pressure gage inside the instrumentation van. At the instant the gage indicated the desired pressure, an overall noise level and a one-third-octave band sound pressure spectrum were obtained with the real-

time spectrum analyzer set for an averaging time of 1/2 second. During this time period, the variation of the jet velocity was no more than 2 percent of the averaged value. At the same instant, total temperature inside the tank was obtained. The total pressure and total temperature measured inside the tank were used in the one-dimensional compressible flow equation to compute the nozzle-exit mean velocity.

RESULTS AND DISCUSSION

From the standpoint of a community, noise radiated directly below an aircaft is of considerable importance. In this discussion, then, the acoustic data obtained directly beneath the upper-surface-blowing model will be given primary consideration.

Spectral Similarity

In this study, several experimental parameters including nozzle aspect ratio, flow-run length, flap-deflection angle, and nozzle-exit velocity were investigated. It is desirable to be able to establish the gross similarity of the radiated noise in terms of the nozzle flow and geometrical parameters. Establishment of spectral similarity requires that an appropriate form of Strouhal number be chosen. One form of Strouhal number based on local flow velocity and length scale was used in references 3 and 12 to show data similarity. In practice, however, the local scale and velocity are unknown for an arbitrary flow configuration associated with upper surface blowing. In an attempt to circumvent the difficulties introduced by these unknowns, a Strouhal number based on the geometrical shield length and nozzle-exit velocities is used in this study. The flow-run length ℓ is taken to be the relevant geometrical length, and the nozzle-exit velocity V_j is taken to be the typical flow velocity. These new scales were chosen because the new mechanism for additional noise radiation which occurs when a wing flap is introduced into jet flow must result from the adjustment which the flow undergoes in order to accommodate the flap. A Strouhal number based on criteria similar to those used in this study has long been used in establishing spectral similarity for subsonic jet noise.

Figure 5 shows noise spectra normalized with respect to the overall noise and plotted against a nondimensional frequency parameter S, where $S = f\ell/V_j$. In figure 5(a), data are plotted for ℓ/h = 4.29, 8.51, and 17; V_j = 174 and 253 m/sec; and $\delta = 0^\circ$. In figure 5(b), data are plotted for ℓ/h = 8.51 and 17; V_j = 174 and 253 m/sec; and $\delta = 30^\circ$. Data are not presented for $\delta = 60^\circ$ because a plot of these data showed considerable scatter. The data scatter is believed to be the result of flow separation from the flap surface due to the large turning angle.

It can be seen that these flyover noise data collapse quite well. Some of the spectra seen in these figures were measured with the flap trailing edge terminated within the potential core region of the wall jet flow ($\ell \leq 10h$), and a discrete tone was clearly evident in one of the spectra used to plot figure 5(b). However, since the discrete tone radiation probably originates from a different mechanism, the tonal component was discounted from the overall noise

in plotting the spectral data in figure 5. The tonal component was discounted by interpolating the one-third-octave band sound level at the band where the discrete tone exists, and by assuming the spectrum is otherwise broadband. The OASPL was then recalculated by using the interpolated one-third-octave band value.

Further comparison of figures 5(a) and 5(b) shows that flap-deflection angle influences both peak frequency and spectral decay at frequencies higher than the peak. For $\delta = 0^\circ$, the peak frequency is at $S = 0.8$, whereas for $\delta = 30^\circ$, the spectral peak occurs at $S = 1.6$. The spectral slopes for low-frequency noise vary as $S^{1.7}$ and $S^{1.2}$ for $\delta = 0^\circ$ and $\delta = 30^\circ$, respectively. For high frequencies, however, the spectral slopes are S^{-2} and $S^{-2.5}$ for $\delta = 0^\circ$ and $\delta = 30^\circ$, respectively.

Normalized one-third-octave band flyover noise spectra are given in figure 6 for the aspect-ratio-50 nozzle. These data are plotted for various values of ℓ/h and δ at $V_j = 174$ and 253 m/sec. It is again evident from figure 6 that the normalized spectra collapse reasonably well for the range of experimental parameters studied. For this relatively high aspect ratio nozzle, figure 6 reveals that the spectral characteristics of the flyover noise are rather insensitive to flap-deflection angle. The spectral peaks occur at approximately $S = 1.3$, and the spectral slopes are S^2 and S^{-2} for low and high frequencies, respectively, for all three values of δ tested.

It should be noted that the flyover noise spectra measured for different flap-deflection angles are not entirely independent of each other. This dependence results because the noise directivity of upper-surface-blowing configurations tends to rotate with the flap deflection. (See ref. 1.) This condition is true provided that flow attachment is insured at the flap trailing edge. Thus, noise spectra measured at $\gamma = 90^\circ$ for $\delta = 0^\circ$ can be expected to be comparable with noise spectra measured at $\gamma = 120^\circ$ for $\delta = 30^\circ$.

When the rotation of noise directivity just discussed is considered, the difference in flyover noise spectra measured for different flap-deflection angles may be interpreted as a variation of noise spectra with azimuthal angle γ. The results obtained with the aspect-ratio-10 nozzle thus indicate a strong directivity effect on the spectra measured, whereas spectra obtained with the aspect-ratio-50 nozzle show no noticeable directivity effect.

To establish the validity of the present experimental technique involving use of a blowdown method, a comparison was made between the present data and similar spectral measurements made by Grosche (see ref. 5) in an anechoic chamber using continuous flow. The measurements in reference 5 were made with an aspect-ratio-23 nozzle and a plate having $\ell/h = 50$ with a zero flap-deflection angle. The jet flow was exhausted parallel to the upper surface of the plate with the jet center line displaced by a distance 0.55h. Although the flow arrangement used in reference 5 was slightly different from the arrangement used in this study, the difference is not considered significant enough to change the overall characteristics of the noise spectra. The curves in figure 7 are the mean curves of figure 5(a) ($w/h = 10$, $\delta = 0^\circ$) and figure 6 ($w/h = 50$, $\delta = 0^\circ$). The data from reference 5 and the data from this study are in good agreement except at low frequencies.

As was mentioned earlier, some of the noise spectra measured in this study contain discrete tones. Although narrowband analyses were not performed at the various operating conditions, these tones could be clearly heard during the data collection process. The common features of these tone radiations are summarized: (1) tone radiations were observed only when the flap trailing edge terminated within the potential core region of the wall flow ($\ell/h \leq 10$); (2) tone radiations were observed only at the highest nozzle-exit velocity tested ($V_j = 253$ m/sec); and (3) with the lowest aspect ratio nozzle (w/h = 10) discrete emissions only occurred with nonzero flap-deflection angle, while with the highest aspect ratio nozzle (w/h = 50) tone radiation occurred with both zero and nonzero flap angles.

Observations of tone radiation for zero flap angle have also been reported by other investigators. (See refs. 3 and 19.) In reference 3, the mechanism for such tone radiation was attributed to the breakdown of the laminar sublayer adjacent to the flap surface. In reference 19, the mechanism responsible for tone radiation was suspected to be the free shear-layer instability as suggested by shadowgraphs that were taken of the flow field. Shadowgraphs of similar flow instabilities were also reported in reference 21.

Figure 8 presents a typical spectrum containing a discrete tone emission obtained during the present study for the aspect-ratio-10 nozzle. Although not shown here, some of the spectra obtained exhibited higher harmonics as well. A simple calculation was made to check the possibility that the tone radiations could have resulted from an acoustic feedback mechanism. This calculation indicated that the most plausible feedback loop seems to consist of flow instability convected downstream to the trailing edge and acoustic radiation from the trailing edge transmitted upstream to the nozzle exit through ambient air.

The dependence of overall sound pressure level on flow Mach number for cases both with and without tone radiation is shown in figure 9. Data are presented for the aspect-ratio-10 nozzle with $\delta = 30^\circ$, $\ell/h = 8.51$ (tone present), and $\ell/h = 17$ (no tone present). It can be seen that when the tone was present, the noise level increased sharply and had a near 10th power dependence on flow Mach number as compared with a typical 5th to 6th power dependence in the absence of discrete tone. Although the mechanism for the tone radiation observed cannot be precisely identified, the mechanism would probably be of little concern in real engine-over-the-wing applications since much rougher flow conditions would exist in an engine exhaust than in the nozzle flow. Indeed, no discrete tones were present in the large-scale aircraft tests reported in reference 20.

Comparison of Present Data With Prediction

A number of theoretical and semiempirical approaches have been made in the past to predict the noise associated with upper-surface-blowing arrangements. For example, in reference 3, Hayden postulated the major mechanism for an undeflected upper-surface-blowing flap as dipoles acting near the flap trailing edge. Using the acoustic data given in reference 3, Hayden also proposed a universal far-field noise spectrum for an upper-surface-blowing flap with zero flap-deflection angle. (See ref. 12.) In Hayden's semiempirical prediction scheme,

the appropriate length scale is taken as the thickness of the characteristic boundary layer. He also predicts the variations in far-field spectra. These variations depend on whether the flap trailing edge ends in the potential core region, in the characteristic decay region, or in the radial decay region of the wall flow.

Working from a physical argument similar to ones already discussed, Fink postulates that the noise radiated by upper-surface-blowing configurations consists of free jet mixing noise, scrubbing noise, and trailing-edge noise. (See ref. 22.) He proposes a step-by-step empirical scheme to calculate the far-field noise spectra.

Filler based his study on the theoretical model developed in reference 10. (See ref. 23.) He proposed a semiempirical scheme for predicting upper-surface-blowing noise. This scheme takes into account the forward-speed effects of the aircraft as well as the location of the jet exit relative to the flap.

Some interesting additional features distinguish the three prediction schemes discussed above. In references 12 and 22, Hayden and Fink use 6th and 5th power dependence of OASPL on trailing-edge velocity, respectively. Filler, on the other hand, uses a 5th power dependence of OASPL on nozzle-exit velocity. In their predictions of noise spectra, the three authors use different length scales to define Strouhal number. In reference 12, Hayden uses a characteristic thickness of the flow at the trailing edge. Fink, however, uses an equivalent nozzle-exit diameter which corresponds to the diameter of a circular nozzle having identical exit area. In reference 23, Filler uses the hydraulic diameter of the nozzle. Hayden, Fink, and Filler also differ in their use of velocity to calculate Strouhal number; Hayden and Fink use trailing-edge velocity, whereas Filler uses nozzle-exit velocity.

In an attempt to test the prediction schemes discussed previously, predicted noise spectra were computed by using the methods given by Hayden, Fink, and Filler. Nozzle-plate configurations tested with a nozzle-exit velocity of 253 m/sec and zero flap-deflection angle are used as examples. Spectral comparisons between the present data and the prediction reported by Hayden in reference 12 for the aspect-ratio-10 nozzle are plotted in figures 10(a) and 10(b) for $\ell/h = 8.51$ and $\ell/h = 17$, respectively. The abscissa is a nondimensional frequency parameter used in reference 12. The data points plotted in figure 10(a) and the corresponding overall sound pressure level were measured with the flap trailing edge terminated in the potential core region of the jet flow ($\ell/h \leq 10$). Figure 10(b) shows spectral data and overall sound level for the aspect-ratio-10 nozzle taken with the trailing edge in the characteristic decay region ($10 \leq \ell/h \leq 40$). Inspection of these figures indicates that correlation between measurement and prediction is rather poor. Although the locations of the spectral peaks varied with the predicted trend, the spectral levels are generally overpredicted, especially at the intermediate frequencies. The disagreement observed between the measured and predicted data may result from a more uniform flow pattern expected for the nozzle described in reference 3. The uniform flow pattern is attributable to the large contraction ratio (160) used. In the present study, the effective contraction ratio is about 4; in addition, the predicted spectra are narrower in effective bandwidth and have steeper slopes.

This type of spectral behavior is normally found in jet noise associated with very uniform exit flow.

Figure 11 gives comparisons between spectral data measured in this study and predictions obtained from Fink's scheme. Data are presented for the aspect-ratio-10 nozzle with $\ell/h = 8.51$ and $\ell/h = 17$ in figures 11(a) and 11(b), respectively. Fink's prediction appears to be reasonably good, especially as shown in figure 11(b) with $\ell/h = 17$. It can be seen that the measured and predicted overall sound pressure levels agree well also.

Figure 12 compares some of the data of this study with predicted data calculated with Filler's scheme, zero forward velocity being assumed. Again, experimental data are presented for the aspect-ratio-10 nozzle with $\ell/h = 8.51$ and $\ell/h = 17$ in figures 12(a) and 12(b), respectively. These figures show that the measured and predicted data do not compare well. The lack of agreement may be due to the fact that the empirical constants used in Filler's prediction were obtained from experimental data taken with a D-shaped nozzle.

The preceding comparisons made between experimental noise spectra and calculated results based on the existing prediction schemes clearly indicate that the extent of agreement may vary from scheme to scheme. The accuracy of each scheme, even when it is valid, may require improvement, however. The present comparisons also reveal the need for further refinements in the existing noise prediction methods for upper-surface-blowing configurations.

Effects of Acoustic Shielding

The possibility of exploiting the shielding effect associated with engine-over-the-wing configurations to reduce the level of flyover noise has gained considerable interest. The amount of reduction of sound intensity perceived by a receiver when a shield is placed between him and the source depends on several factors; namely, the spatial and spectral distribution of the source, the ratio of the sound wavelength to the dimension of the shield, and relative positions of the source and receiver to the shield. For the simple case of a small source emitting short wavelength sound compared with the shield dimension, substantial reduction of sound may be achieved when the direct path is interrupted by the shield.

In the case of upper-surface-blowing noise, one can argue that the spatial distribution of noise sources may be divided into two categories: (1) the primarily high frequency noise source (with wavelength comparable to or smaller than the plate dimension) located in the upper free shear layer; and (2) the relatively low frequency noise source emitting sound in the near-wake flow downstream of the flap trailing edge. For a given velocity at the nozzle exit, the spectrum and strength for source (1) is nearly independent of the flap length. For source (2), however, the strength varies with the local velocity in the near wake, which in turn varies inversely with the flow-run length of the plate. The typical frequency of sound radiated from source (2) also varies inversely with the flow-run length. This understanding was essential in the selection of the method used to evaluate acoustic shielding discussed in this paper.

Grosche (see ref. 5) conducted an extensive experimental investigation to evaluate the acoustic shielding accomplished with a high-aspect-ratio turbulent jet in the proximity of a flat plate. More recently, Von Glahn, Groesbeck, and Reshotko (see ref. 17) carried out an experiment similar to that performed in reference 5. In both experiments, the distance between the jet center line and the flat plate was varied. In his evaluation of the shielding effect, Grosche compared the noise directivities in the upper half space of the plate with those of the lower half space of the plate. However, Von Glahn, Groesbeck, and Reshotko obtained noise measurements directly below the flap surface and compared these data with corresponding data obtained with the nozzle alone. The principal conclusions derived from both sets of experiments are similar. Namely, (1) for a fixed separation distance between the nozzle and plate, the benefits of shielding increase when either the plate length or the jet velocity is increased; and (2) for constant plate length and jet velocity, shielding increases as the jet is moved away from the plate until maximum shielding is attained. On the other hand, the overall shielding observed when the jet is either close to or attached to the plate is much less significant.

From aerodynamic considerations, displacement of the jet flow above the plate would translate to a reduction in powered-lift performance (no attached flow). Thus, in considering the acoustic shielding effect of an upper-surface-blowing system, the investigator should restrict himself to the case where the jet flow is very close and attached to the shield surface. Evaluation of acoustic shielding performed by comparing noise radiated directly below a nozzle with and without a shield may not be realistic since the nozzle-alone configuration is not applicable to a powered-lift aircraft. Furthermore, the noise mechanisms associated with an upper-surface-blowing system differ from those in a free turbulent jet.

In analyzing the data given in this section, considerations were given to the ultimate choice of baseline data for evaluating the acoustic shielding achieved with the nozzle-plate arrangement. Because of the additional (in fact, dominant) low frequency noise source introduced when a plate is brought into contact with the jet flow and because the source is dependent on flow-run length, only the high frequency noise component radiated from the upper free shear layer suffers the plate shielding. The low frequency noise component radiated from the downstream trailing-edge wake is affected by the plate diffraction only. Since this downstream source is located near the flap and is symmetrical to it, the diffraction effect would be expected to be the same both above and below the flap. Theoretical analyses based on simplified physical models have been reported in references 3, 4, and 21 which give direct support of this view.

Based on the reasoning above, the decision was made to evaluate the shielding effects in terms of Δ dB obtained by subtracting the noise measured directly below the model from corresponding measurements made above the model. By so doing, the noise contribution from the trailing-edge wake and its diffraction effect should nearly cancel; thereby a net difference which reflects the shielding of the free shear-layer noise by the plate is left. This method appears to be adequate for a flat plate.

When the flat plate is replaced by a turning flap, however, the directivity has been found to turn by roughly the same amount. (See ref. 1.) Consequently,

the argument given would no longer hold unless an added correction is made to account for flap turning. The required correction may be estimated from the theoretical directivity of the trailing-edge noise as predicted in references 3 and 4 when the amount of turning in directivity is assumed to be the same as the flap angle. The theoretical directivity applicable in the present situation for nonzero flap angle is given by

$$D(\gamma) \approx \sin^2 \frac{\gamma - \delta}{2}$$

Therefore, the correction factor needed to account for flap turning angle is

$$\Delta dB_\delta = 10 \log_{10} \frac{\sin^2\left(\frac{\gamma - \delta}{2}\right)}{\sin^2\left(\frac{\gamma}{2}\right)}$$

Application of this correction to the present data also provides an indirect check on the validity of the theoretical directivity used.

Comparison of Overall Sound Pressure Levels

Figure 13 illustrates the ΔOASPL variation with nondimensional flow-run length ℓ/h for the aspect-ratio-10 nozzle at two velocities (V_j = 174 m/sec and V_j = 253 m/sec) and flap-deflection angles ($\delta = 0^\circ$ and $\delta = 30^\circ$). In the case of $\delta = 0^\circ$, figure 13(a) shows the difference in ΔOASPL to be rather small, on the order of 2 dB. The trend is somewhat expected; that is, ΔOASPL increases at the higher values of ℓ/h. In figure 13(b), with $\delta = 30^\circ$, the data shown have not been corrected for directivity rotation. If corrected by using the expression given, the ΔOASPL values expected for $\delta = 30^\circ$ in figure 13(b) would be 4 to 5 dB higher than those plotted for $\delta = 0^\circ$ in figure 13(a).

A reasonable confirmation of the trend displayed in figures 13(a) and 13(b) was accomplished by examining data reported by Grosche in reference 5 for the case where the jet center line is 0.55h above a plate with 0° deflection angle. Grosche's data show that the OASPL variation is small (about 3 dB) even for ℓ/h as high as 100. (See fig. 14.) However, additional data presented in reference 5 indicate that the ΔOASPL increases noticeably when the nozzle is moved to greater distances above the plate where the interaction between the flow and flap trailing edge diminishes.

These observations indicate that (1) the shielding of the upper free shear-layer noise component has a small contribution to the overall noise perceived directly below the plate, and (2) the expected theoretical trailing-edge noise directivity rotation does not occur.

Comparison of Sound Pressure Spectra

In order to gain thorough insight into the effect of acoustic shielding by blowing over the upper surface of a wing flap, the difference in sound radiated above and below the plate in terms of frequency should be examined.

The method used to sort out the general trends indicated by the present data involves comparisons made by plotting the difference in SPL directly above and below the plate against the nondimensional frequency parameter S, where $S = f\ell/V_j$. The following reasons influenced the choice of these parameters to define S: (1) in an earlier section of this paper it was demonstrated that S appears to be appropriate to collapse the spectral data; (2) the shielding and dominant radiation wavelength depend on ℓ; and (3) the jet velocity is related to the strength of both sources present.

This method of comparison should yield a mean trend which would make a quantitative description of the flap-shielding effect possible. A quantitative evaluation scheme for wing-flap shielding in an upper-surface-blowing configuration has not been attempted in any previous studies.

Figures 15(a) and 15(b) show the variation of ΔSPL with S for the aspect ratio 10 and 50 nozzles, respectively. Data are plotted for a range of values of ℓ/h, δ, and V_j. Noticeable scattering of the data is seen, but this is not unexpected since a single parameter S is used to represent a very complex phenomenon. Nevertheless, the following trends seem to emerge: (1) from $S = 0.5$ to $S = 5$ the ΔSPL variation is rather flat; (2) for $S > 10$, ΔSPL increases rapidly with S; and (3) for $S < 0.5$, ΔSPL increases as S is decreased. These trends appear to be independent of flap-deflection angle. The large ΔSPL values at higher values of S should be attributed to the shielding of high frequency noise emitted in the upper free shear layer near the nozzle exit and above the plate. The lack of appreciable variation in ΔSPL over the intermediate frequency components ($0.5 < S < 5$) seems to support the argument that noise produced near the flap trailing edge is nearly symmetrical and uniform. The increase of ΔSPL as S is decreased below 0.5 is not clearly understood at present.

Noise data obtained with upper-surface-blowing models by other investigators have been examined in a way similar to the method just discussed. Figure 16 was prepared by replotting various spectral data reported in references 5 and 18 to 20. The mean curve obtained from the present data plotted in figure 15(a) is included in figure 16 for comparison. An inspection of figure 16 shows that data reported in reference 5 and 18 agree reasonably well with the mean curve obtained from the present data. The scattering of model data about the mean curve, obtained with present data, at higher values of S is caused primarily by data reported in reference 19. The data taken from reference 20 for a large-scale STOL aircraft show a distinctly different trend than that of the model data. At the higher values of S, the large-scale data indicate that the shielding is nearly 20 dB higher than the mean of the model data. This discrepancy is most likely caused by configuration differences in the large and small-scale models tested. The primary differences are: (1) real turbofan engines rather than jet nozzles were used in the tests reported by Preisser and Fratello in reference 20; consequently, the high frequency part of the spectrum is domi-

nated by aft-end engine noise which could be more effectively shielded by the wing flap; (2) the span-chord ratio of the large-scale flap is several times greater than that used in the present tests; (3) the flap trailing edge of the large-scale model is slanted relative to the nozzle-exit plane, but the two are parallel on the smaller model; and (4) the large-scale model was complete with fuselage whereas the small-scale model consisted of a nozzle and plate only.

SUMMARY OF RESULTS

An investigation has been conducted to determine the effects of acoustic shielding with an upper-surface-blowing model. Acoustic data were obtained for a range of nozzle-exit velocities with slot nozzles having identical exit areas. Tests of various model configurations led to the following results:

1. Similarity exists for noise spectra obtained with the models tested. The appropriate frequency parameter is a Strouhal number based on the nozzle-exit velocity and flow-run length.

2. Discrete tone emissions were found to occur with certain nozzle-plate configurations and operating conditions. The mechanism of this radiation could be related to acoustic feedback between the shear layer at the nozzle exit and the flap trailing edge.

3. Data from the present study were used for comparison with three different prediction schemes. Good agreement was obtained with the prediction scheme given in NASA CR-134883. However, agreement between the present data and prediction schemes reported in NASA CR-2126 and AIAA Paper No. 76-518 was relatively poor.

4. A simple method is proposed to evaluate quantitatively the acoustic shielding of the wing-flap surface to noise radiated directly beneath the model. An empirical curve is established to evaluate the acoustic shielding of noise in terms of frequency. The empirical curve shows fair agreement with experimental data obtained by other investigators. However, large differences which are primarily attributable to turbofan engine aft-end noise were found when comparisons were made with data obtained with a large-scale simulated STOL aircraft.

5. The acoustic shielding was found to increase with Strouhal number. The net benefit of shielding in terms of overall noise, however, is small with a realistic flow-run length.

Langley Research Center
National Aeronautics and Space Administration
Hampton, VA 23665
December 21, 1976

REFERENCES

1. Maglieri, Domenic J.; and Hubbard, Harvey H.: Preliminary Measurements of the Noise Characteristics of Some Jet-Augumented-Flap Configurations. NASA MEMO 12-4-58L, 1959.

2. Grosche, F. R.: Measurements of the Noise of Air Jets From Slot Nozzles With and Without Shields. DLR FB 68-46, Aerodynamische Versuchsanstalt (Göttingen), July 1968.

3. Hayden, Richard E.: Sound Generation by Turbulent Wall Jet Flow Over a Trailing Edge. M.S. Thesis, Purdue Univ., Aug. 1969.

4. Ffowcs Williams, J. E.; and Hall, L. H.: Aerodynamic Sound Generation by Turbulent Flow in the Vicinity of a Scattering Half Plane. J. Fluid Mech., vol. 40, pt. 4, Mar. 1970, pp. 657-670.

5. Grosche, F. R. (D. G. Randall, transl.): On the Generation of Sound Resulting From the Passage of a Turbulent Air Jet Over a Flat Plate of Finite Dimensions. Library Trans. No. 1460, Brit. R.A.E., Oct. 1970.

6. Dorsch, Robert G.; Krejsa, Eugene A.; and Olsen, William A.: Blown Flap Noise Research. AIAA Paper No. 71-745, June 1971.

7. Gruschka, Heinz D.; and Schrecker, Gunter O.: Aeroacoustic Characteristics of Jet Flap Type Exhausts. AIAA Paper No. 72-130, Jan. 1972.

8. Gibson, Frederick W.: Noise Measurements of Model Jet-Augmented Lift Systems. NASA TN D-6710, 1972.

9. Aircraft Engine Noise Reduction. NASA SP-311, 1972.

10. Chase, David M.: Sound Radiated by Turbulent Flow off a Rigid Half-Plane as Obtained From a Wavevector Spectrum of Hydrodynamic Pressure. J. Acoust. Soc. Amer., vol. 52, no. 3 (pt. 2), Sept. 1972, pp. 1011-1023.

11. Hubbard, Harvey H.; Chestnutt, David; and Maglieri, Domenic J.: Noise Control Technology for Jet-Powered STOL Vehicles. ICAS Paper No. 72-50, Aug.-Sept. 1972.

12. Hayden, Richard E.: Noise From Interaction of Flow With Rigid Surfaces: A Review of Current Status of Prediction Techniques. NASA CR-2126, 1972.

13. Hayden, Richard E.: Fundamental Aspects of Noise Reduction From Powered-Lift Devices. [Preprint] 730376, Soc. Automot. Eng., Apr. 1973.

14. Reshotko, Meyer; Goodykoontz, Jack H.; and Dorsch, Robert G.: Engine-Over-the-Wing Noise Research. NASA TM X-68246, 1973.

15. Schrecker, G. O.; and Maus, J. R.: Noise Characteristics of Jet Flap Type Exhaust Flows. NASA CR-2342, 1974.

16. Clark, Lorenzo R.: An Experimental Study of the Noise Field Generated by Jet Flow Blowing Over the Upper Surface of a Simulated Wing and Flap. M.S. Thesis, George Washington Univ., 1974.

17. Von Glahn, U.; Groesbeck, D.; and Reshotko, M.: Geometry Considerations for Jet Noise Shielding With CTOL Engine-Over-the-Wing Concept. AIAA Paper No. 74-568, June 1974.

18. Reddy, N. N.; and Brown, W. H.: Acoustic Characteristics of an Upper-Surface Blowing Concept of Powered Lift System. AIAA Paper No. 75-204, Jan. 1975.

19. Patterson, Grant T.; Joshi, M. C.; and Maus, James R.: Experimental Investigation of the Aeroacoustic Characteristics of Model Slot Nozzles With Straight Flaps. AIAA Paper No. 75-471, Mar. 1975.

20. Preisser, John S.; and Fratello, David J.: Acoustic Characteristics of a Large Upper-Surface Blown Configuration With Turbofan Engines. AIAA Paper No. 75-473, Mar. 1975.

21. Tam, Christopher K. W.; and Yu, James C.: Trailing Edge Noise. AIAA Paper No. 75-489, Mar. 1975.

22. Fink, Martin R.: Prediction of Externally Blown Flap Noise and Turbomachinery Strut Noise. NASA CR-134883, 1975.

23. Filler, L.: Prediction of Far-Field Jet/Trailing-Edge Interaction Noise for Engine-Over-the-Wing Installations. AIAA Paper No. 76-518, July 1976.

TABLE I.- MATRIX OF MODEL GEOMETRIES AND JET VELOCITIES TESTED

Aspect ratio, w/h (a)	Ratio of flow-run length to nozzle height, ℓ/h, for -			Flap angle, δ, deg	Jet velocity, V_j, m/sec
	ℓ = 0.061 m	ℓ = 0.121 m	ℓ = 0.242 m		
10	4.29	8.51	17	0	174
				30	221
				60	253
50	9.60	19.04	38.12	0	174
				30	253
				60	

[a]For aspect ratio w/h of 10, w = 0.142 m and h = 0.014 m; for aspect ratio w/h of 50, w = 0.318 m and h = 0.006 m.

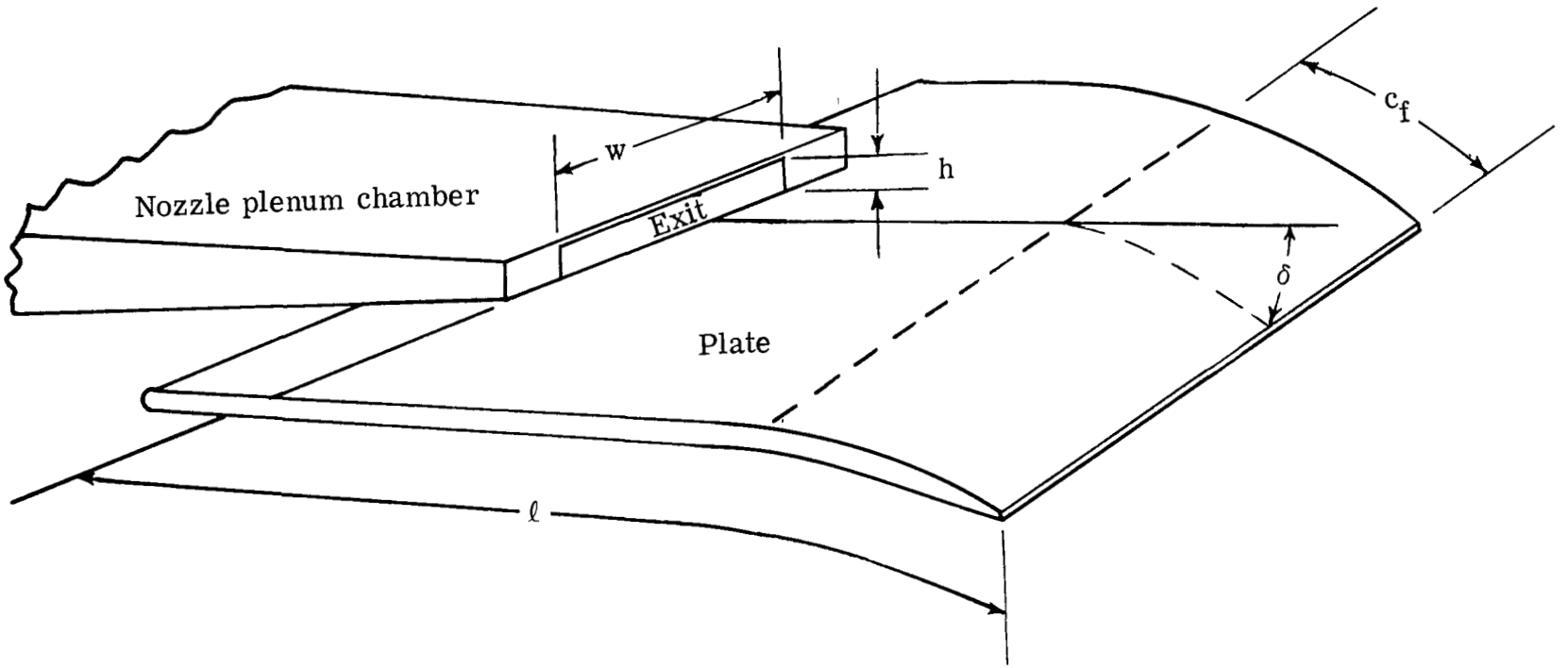

Figure 1.- Diagram of test model with parameters.

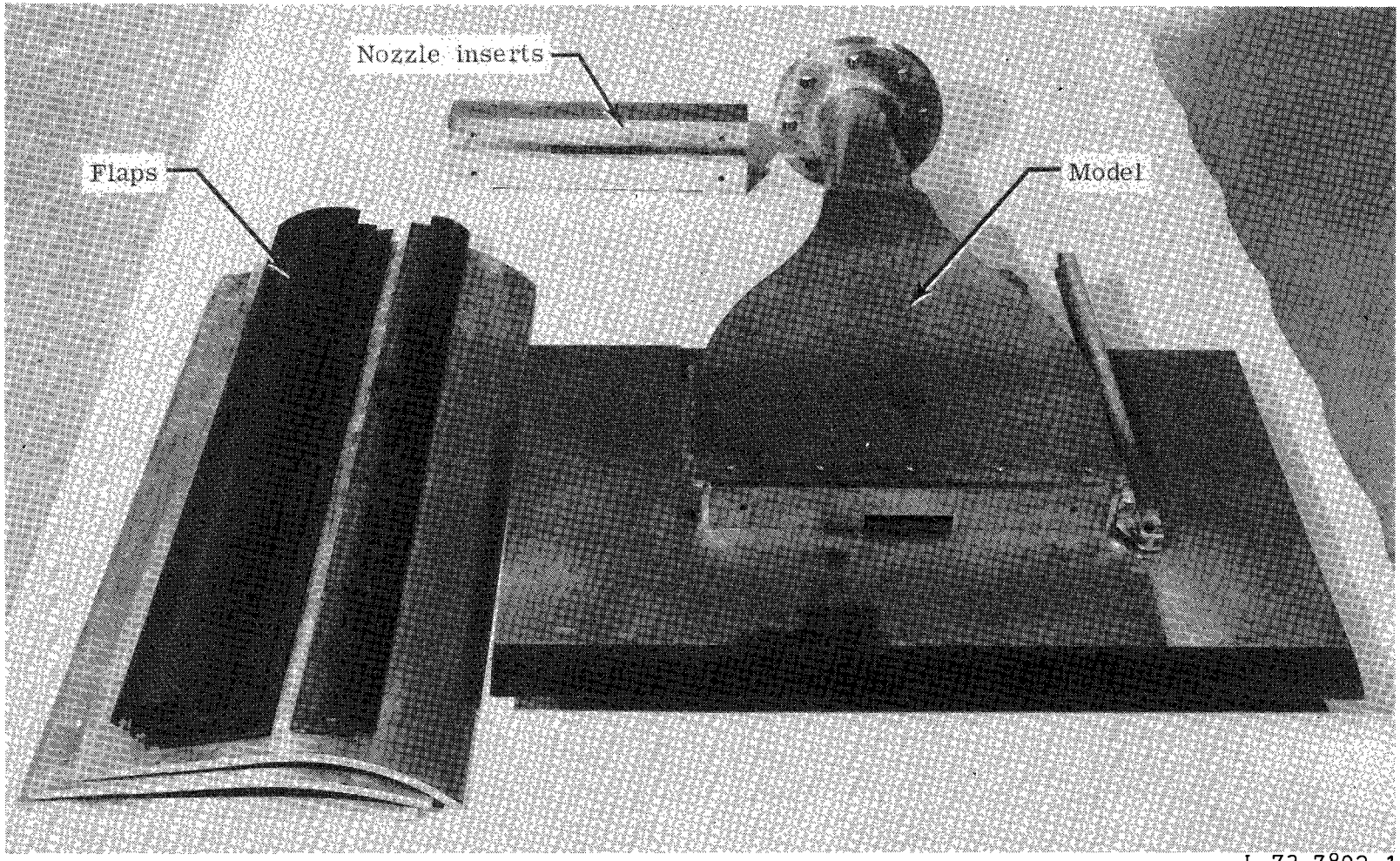

L-73-7802.1

Figure 2.- Photograph of model hardware.

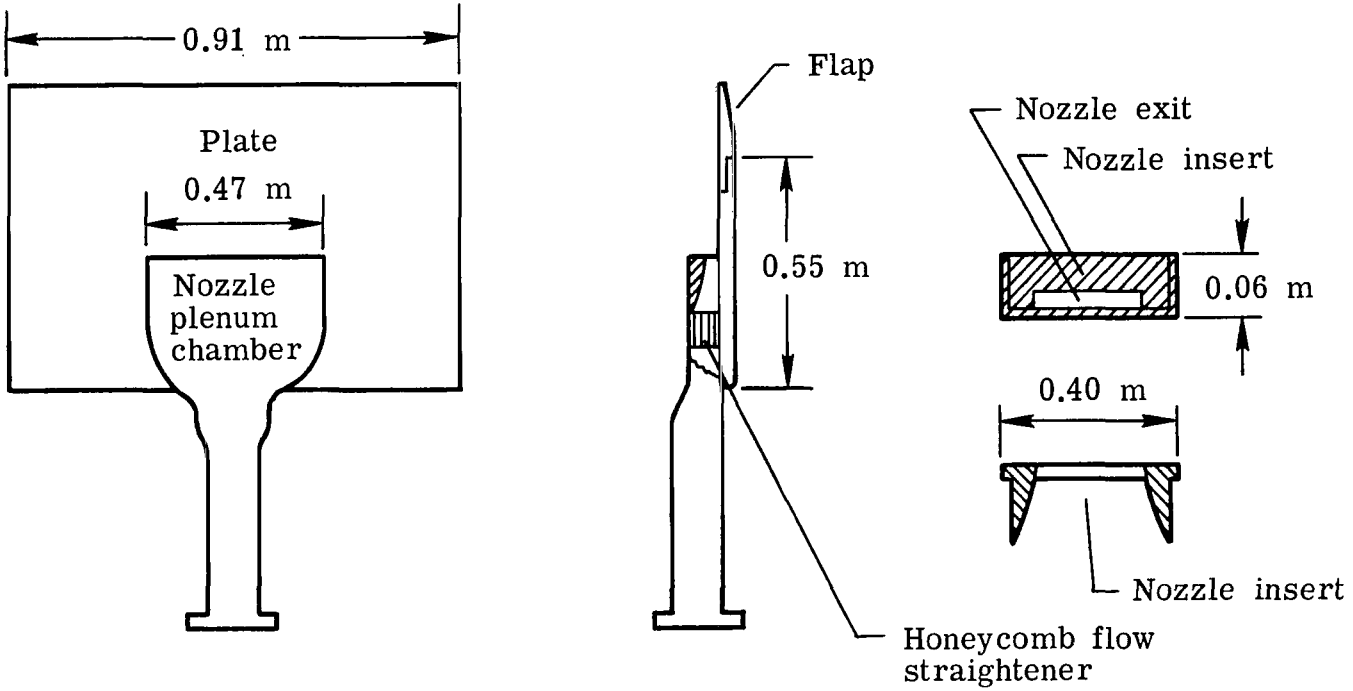

Figure 3.- Diagrams of typical model configuration with dimensions. $\delta = 0^{\circ}$.

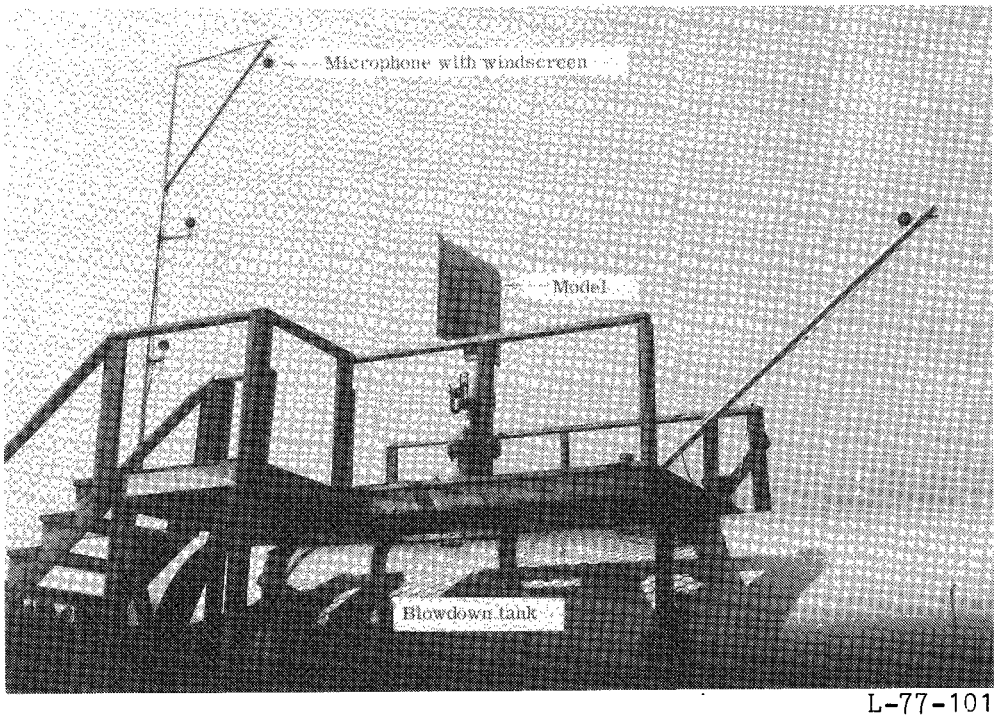

L-77-101

(a) Photograph of test setup.

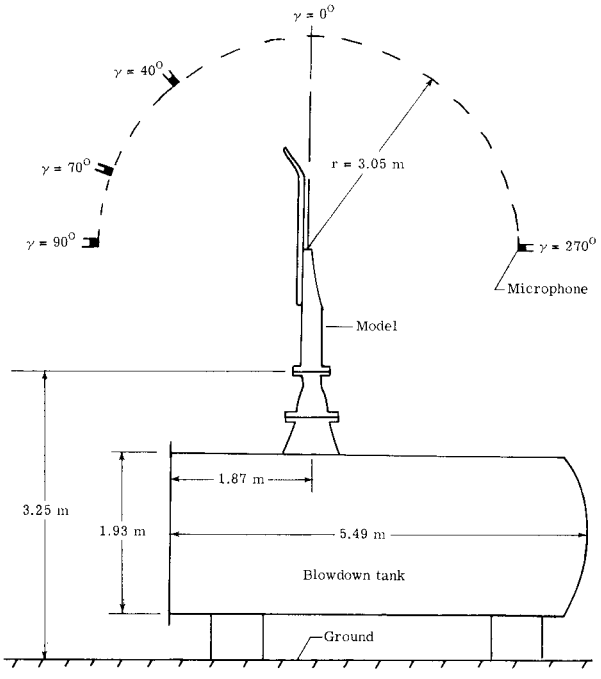

(b) Diagram of test rig with dimensions.

Figure 4.- Photograph and diagram of test setup.

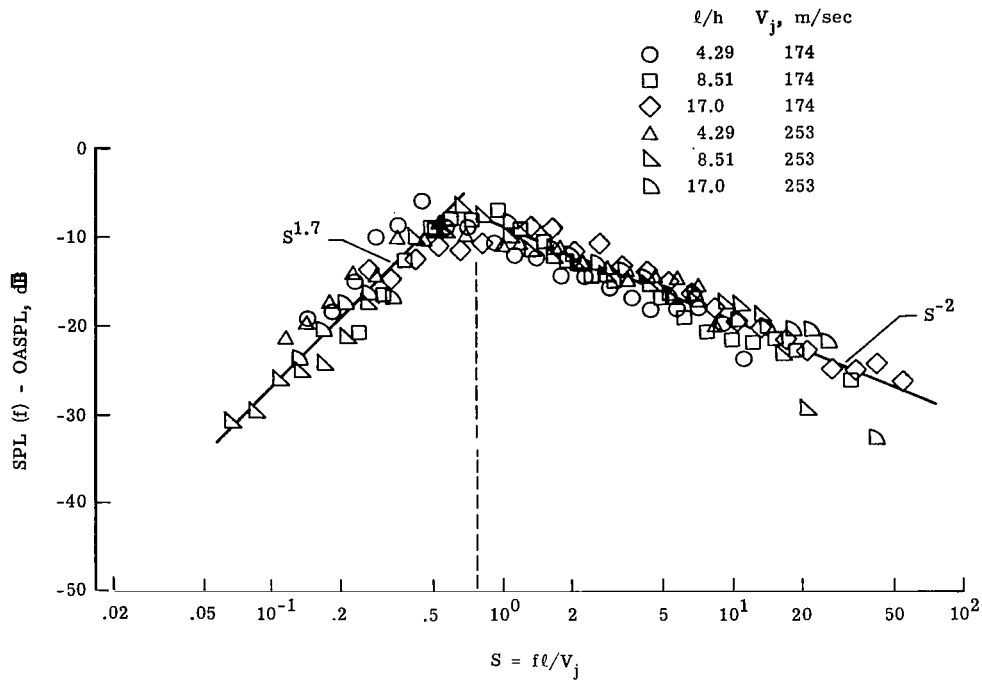

(a) $\delta = 0^{\circ}$.

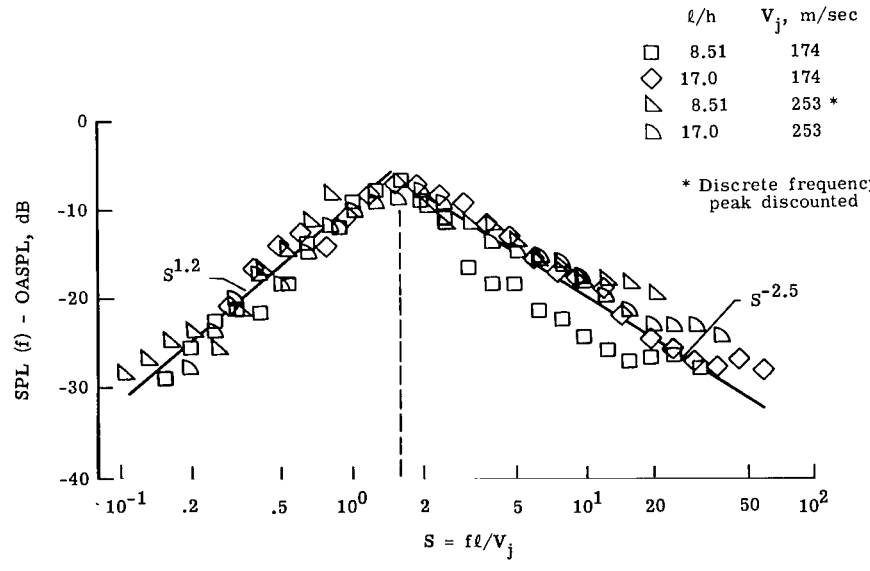

(b) $\delta = 30^{\circ}$.

Figure 5.- Similarity of one-third-octave band spectra; w/h = 10; $\gamma = 90^{\circ}$.

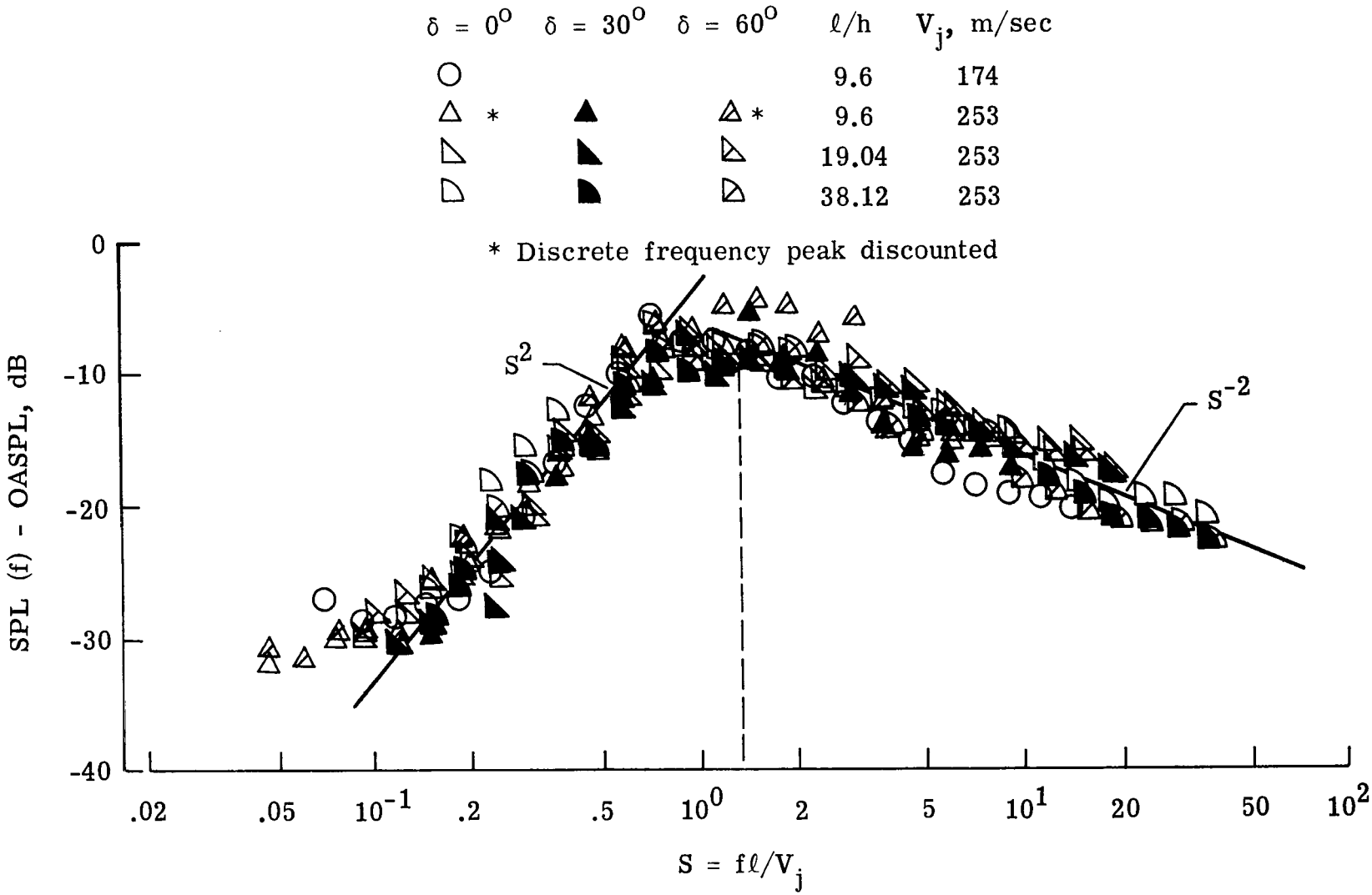

Figure 6.- Similarity of one-third-octave band spectra. w/h = 50; $\gamma = 90^{\circ}$.

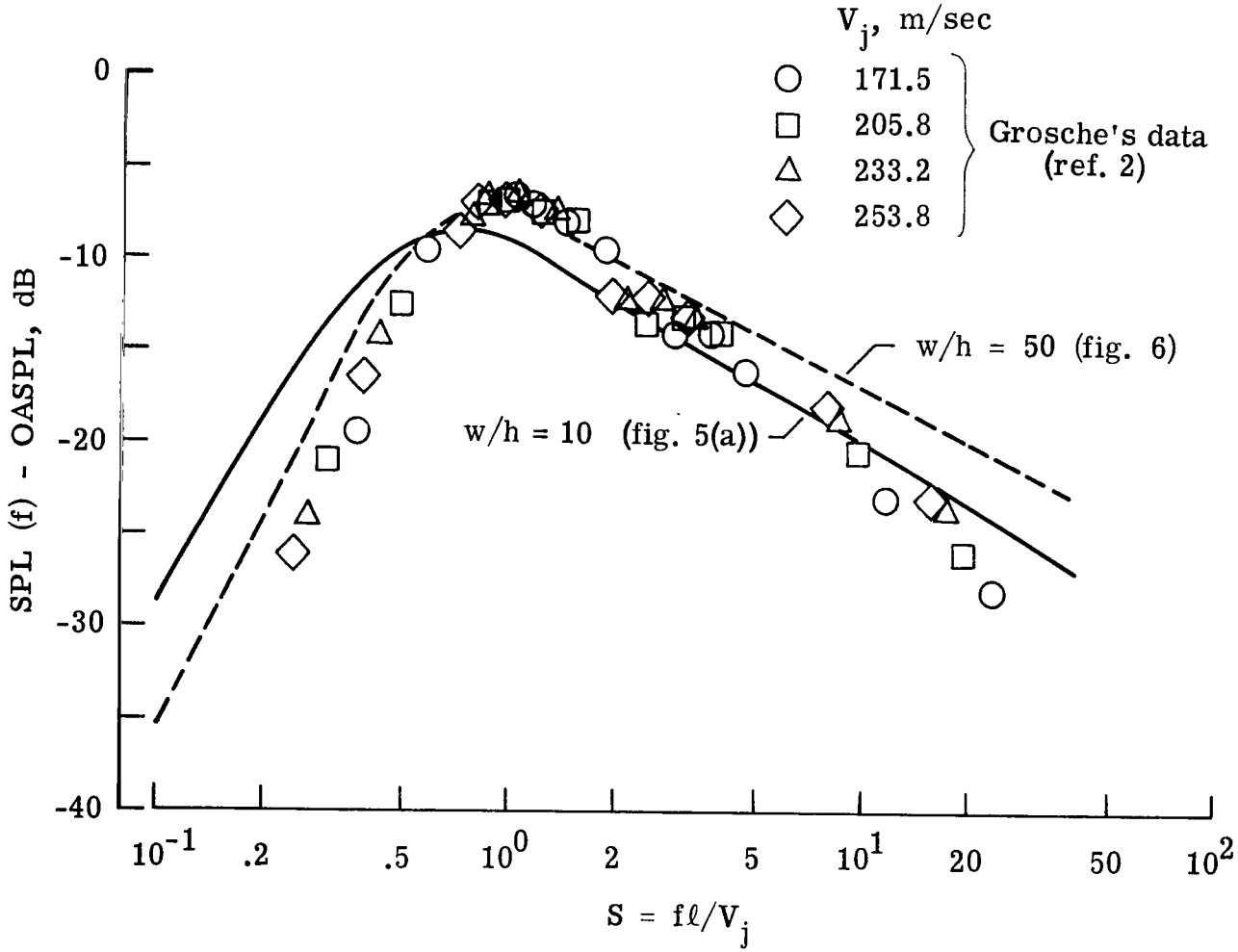

Figure 7.- Comparison of present one-third-octave band data from figures 5(a) and 6 with data reported by Grosche. w/h = 23; ℓ/h = 50; $\delta = 0^{\circ}$; $\gamma = 90^{\circ}$.

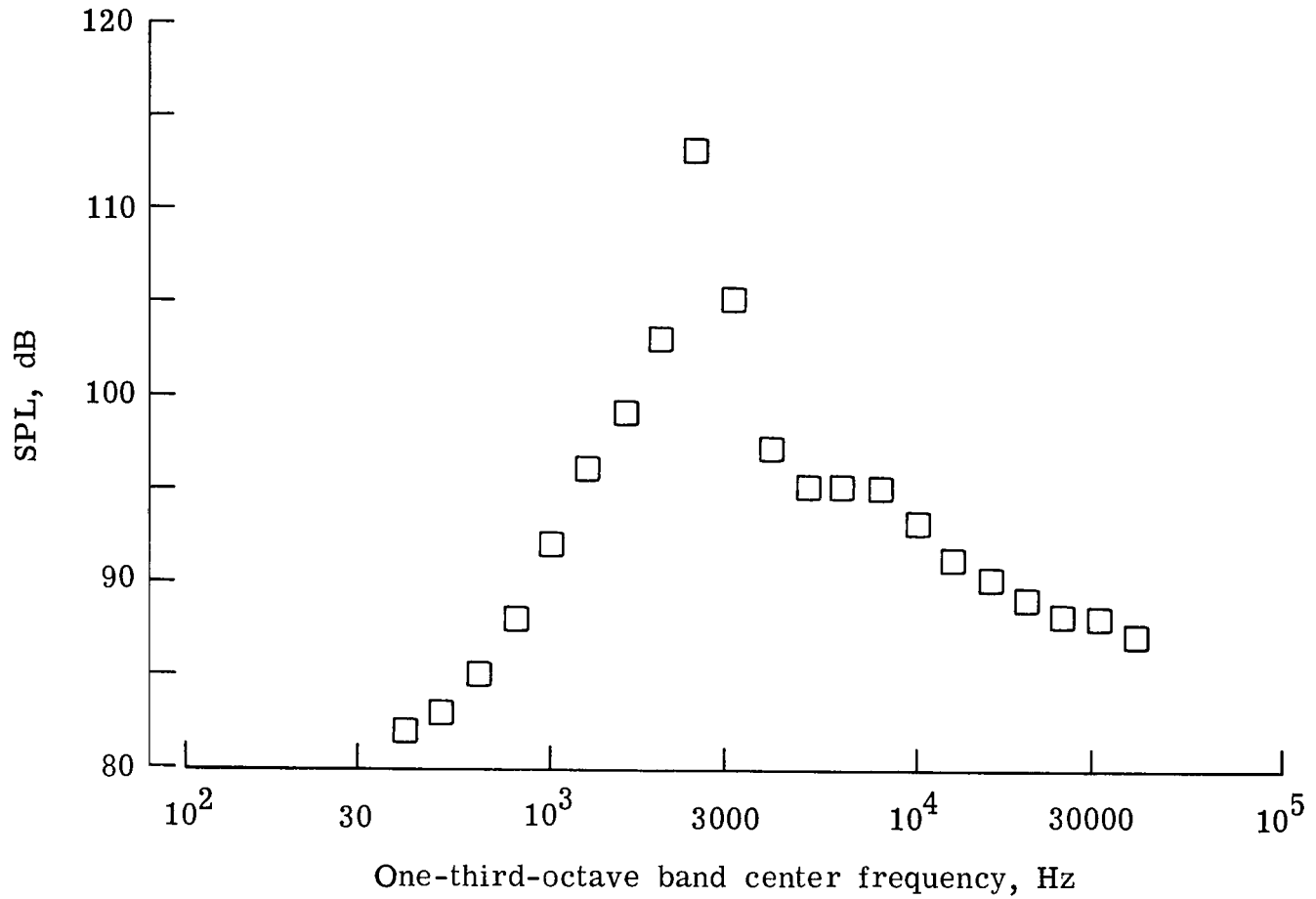

Figure 8.- Spectrum showing discrete tone emission. w/h = 10; ℓ/h = 8.51; $\delta = 30^\circ$; $\gamma = 90^\circ$; V_j = 253 m/sec.

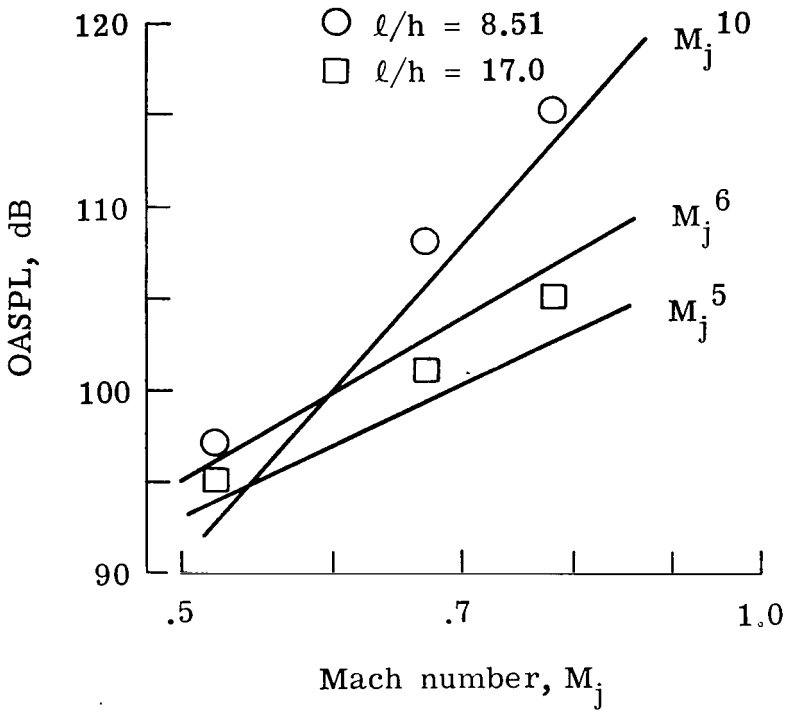

Figure 9.- Variation of overall sound pressure level with flow Mach number. w/h = 10; $\delta = 30^\circ$; $\gamma = 90^\circ$

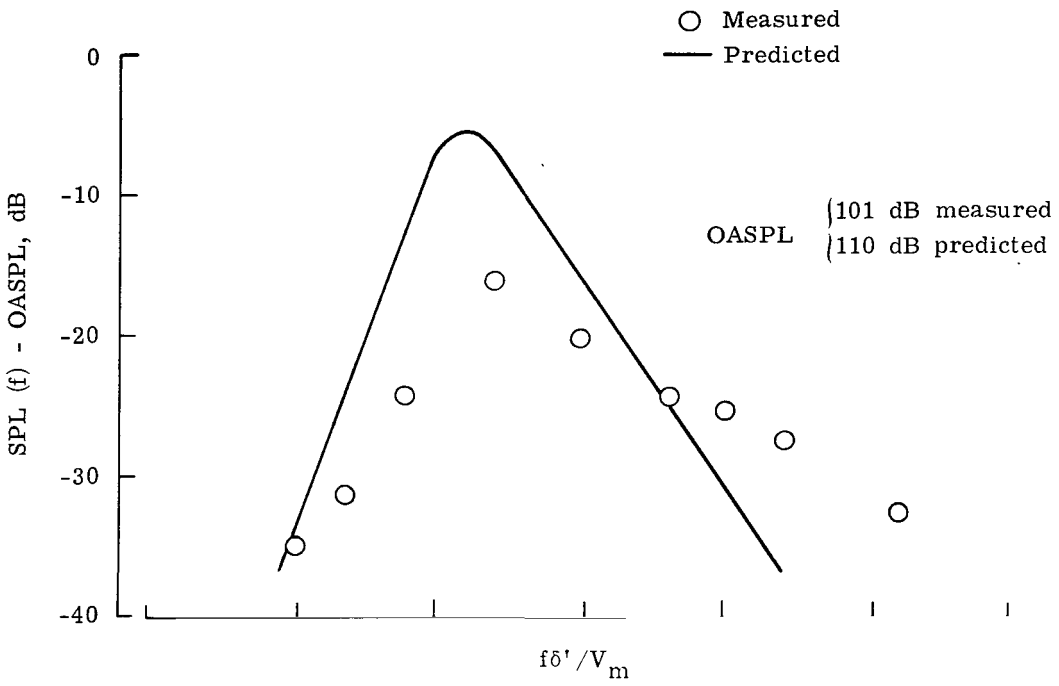

(a) Potential core region; $\ell/h = 8.51$; $V_m = V_j = 253$ m/sec.

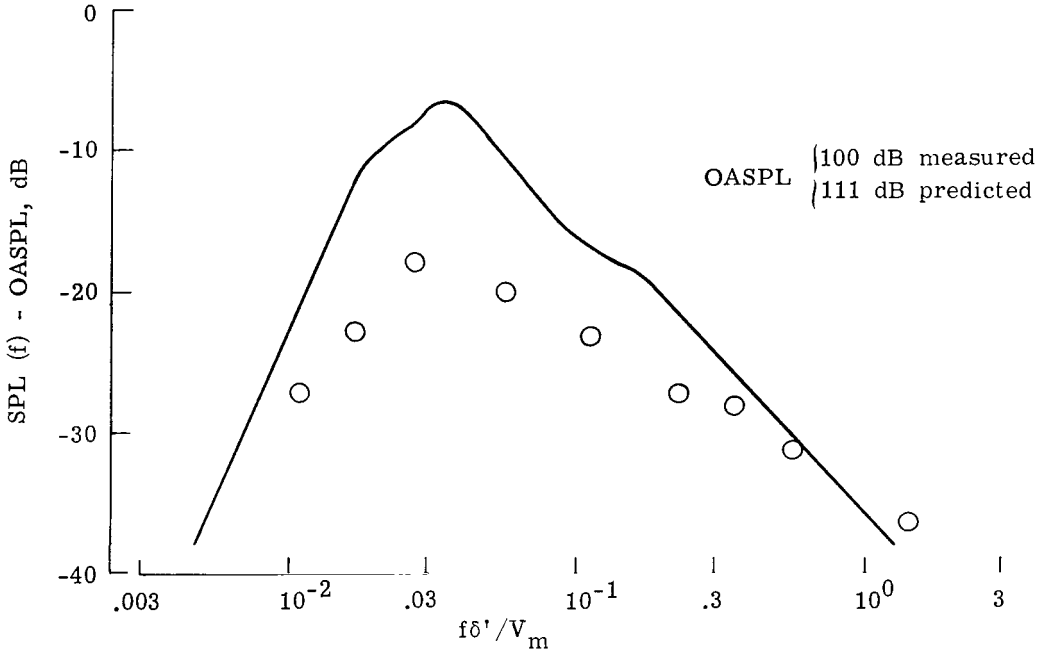

(b) Characteristic decay region; $\ell/h = 17$; $V_m = 223$ m/sec; $V_j = 253$ m/sec.

Figure 10.- Comparison of normalized one-third-octave band data from present study with Hayden's prediction. $w/h = 10$; $\delta = 0^\circ$; $\gamma = 90^\circ$.

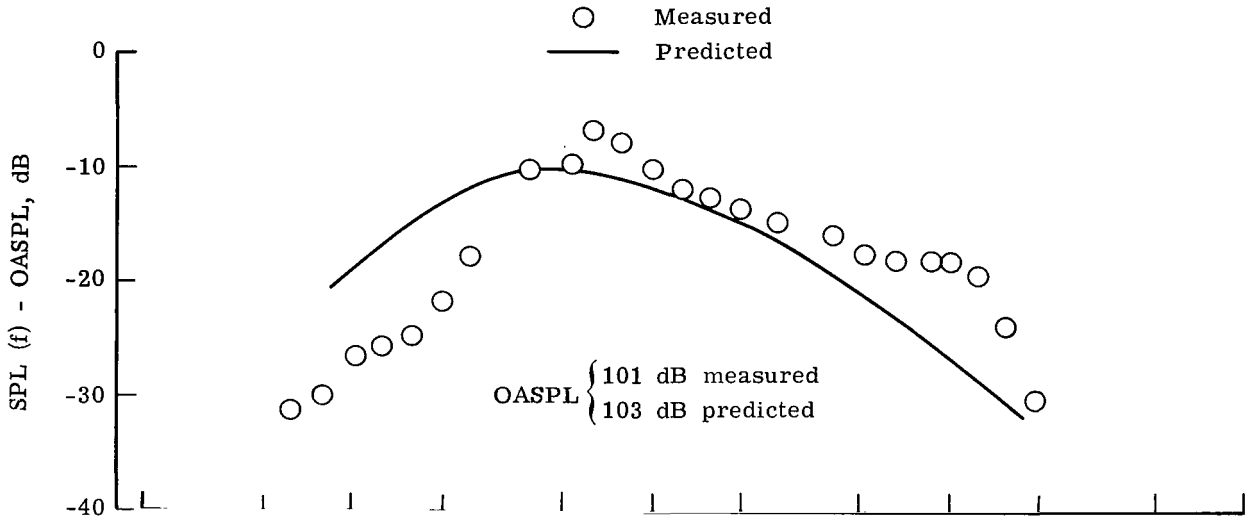

(a) $\ell/h = 8.51$.

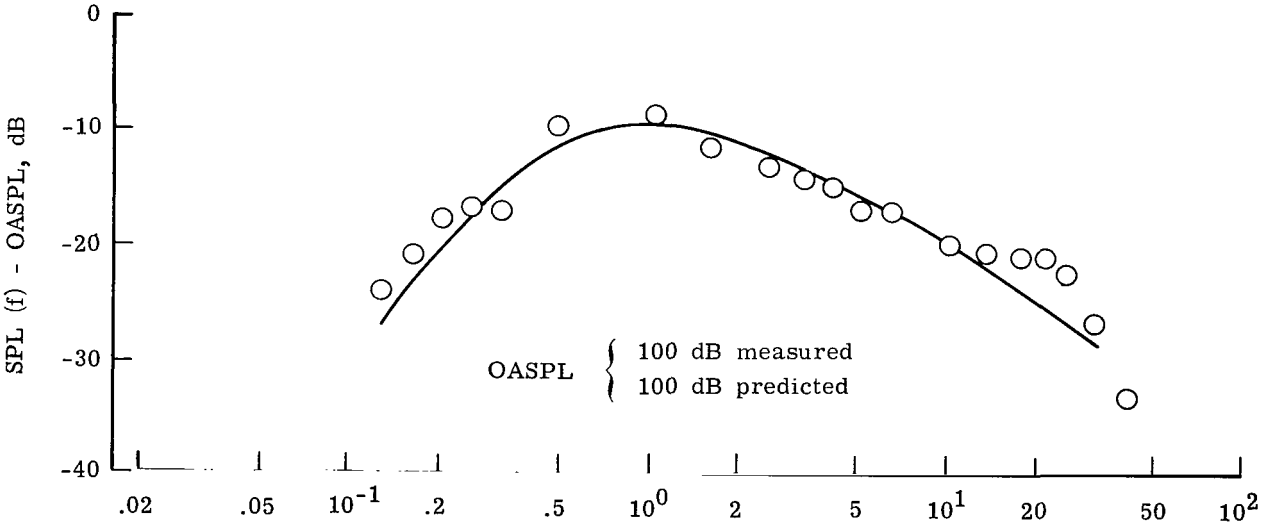

(b) $\ell/h = 17$.

Figure 11.- Comparison of normalized one-third-octave band data from present study with Fink's prediction. $w/h = 10$; $\gamma = 90^{\circ}$; $V_j = 253$ m/sec.

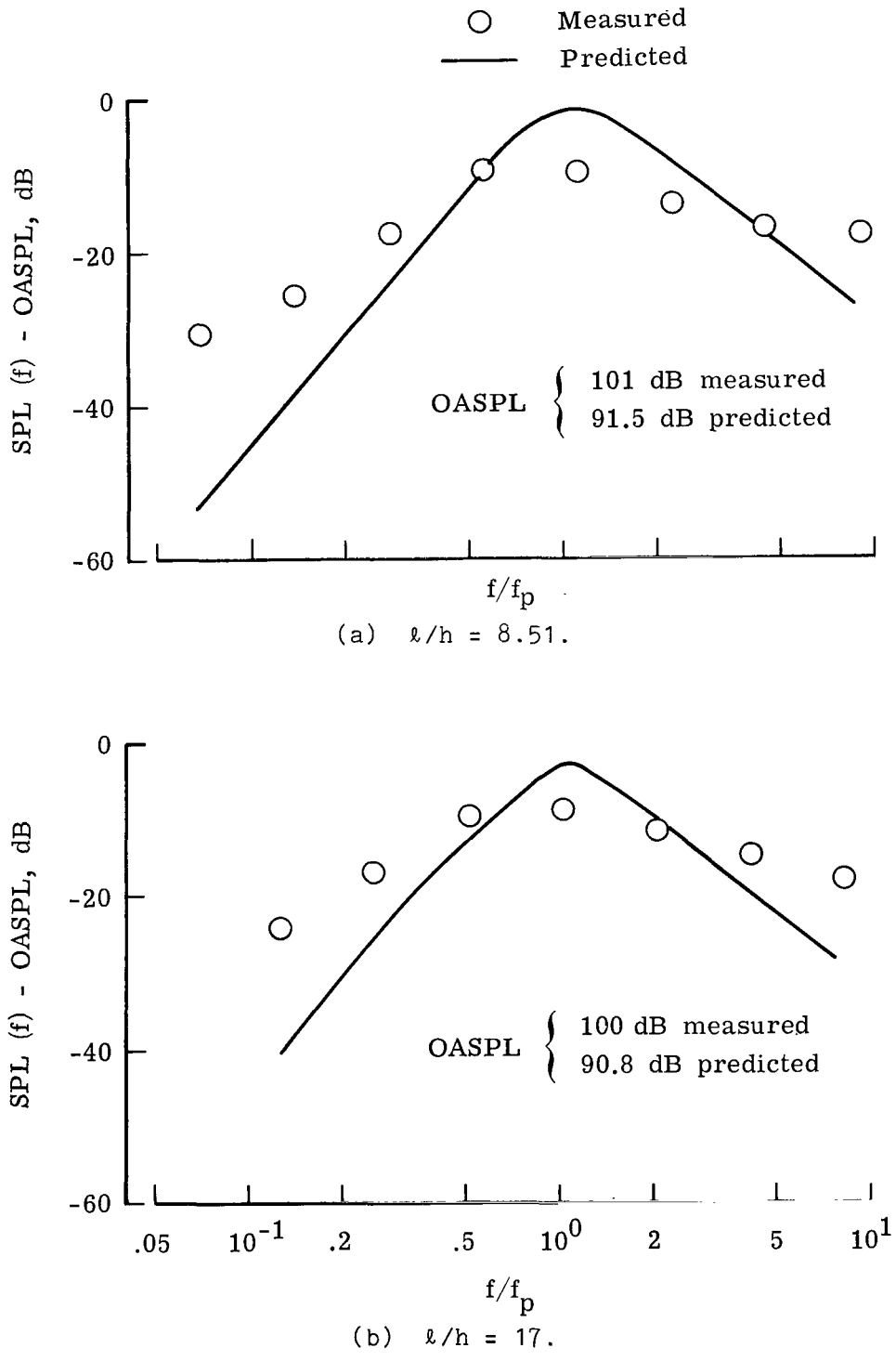

Figure 12.- Comparison of normalized one-third-octave band data from present study with Filler's prediction. w/h = 10; $\delta = 0^{\circ}$; $\gamma = 90^{\circ}$; $V_j = 253$ m/sec.

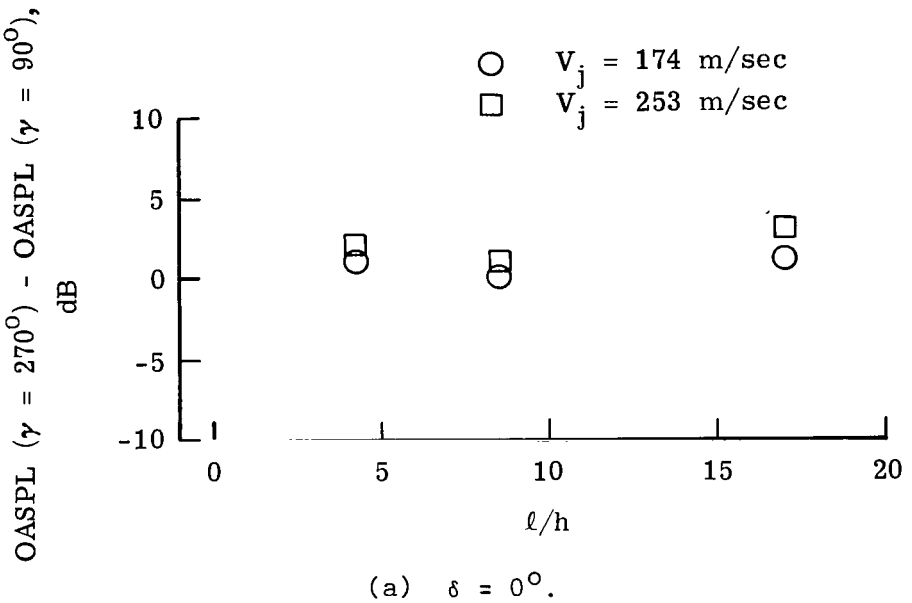

(a) $\delta = 0^{\circ}$.

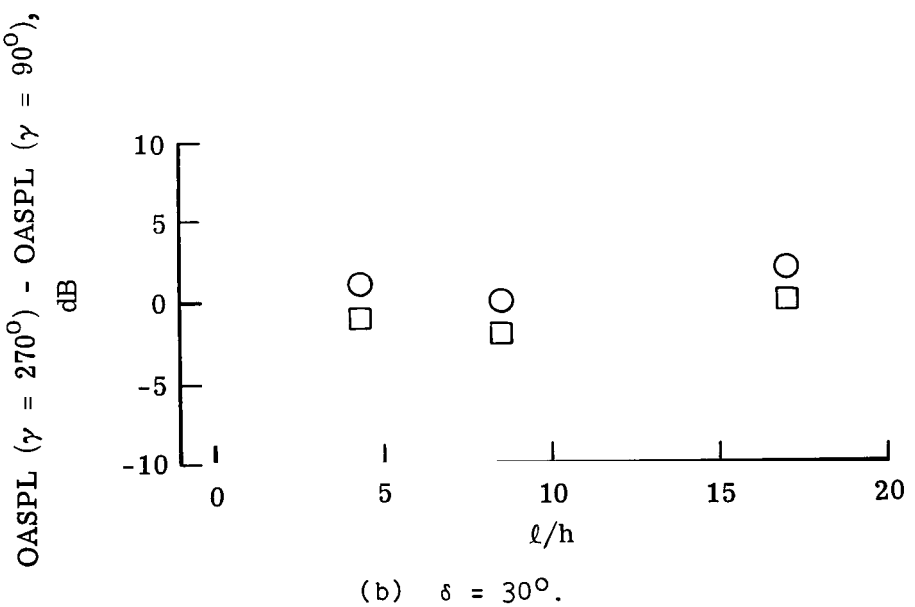

(b) $\delta = 30^{\circ}$.

Figure 13.- Variation of relative overall sound pressure level with ratio of flow-run length to nozzle height. w/h = 10.

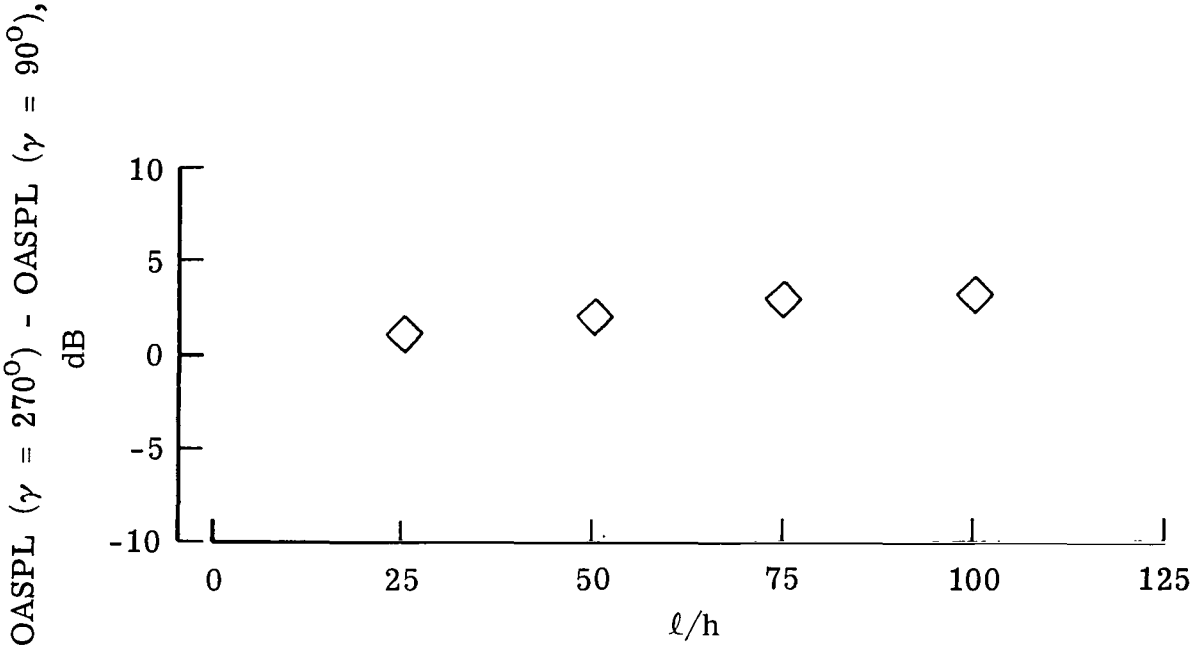

Figure 14.- Variation of relative overall sound pressure level with ratio of flow-run length to nozzle height as reported by Grosche. w/h = 23; $\delta = 0^{\circ}$; V_j = 329 m/sec.

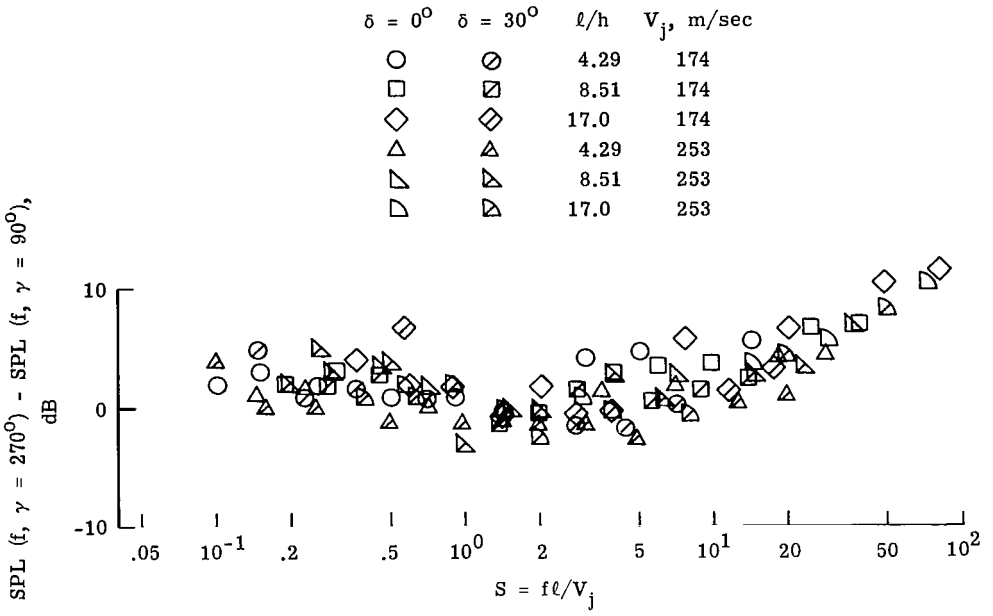

(a) w/h = 10.

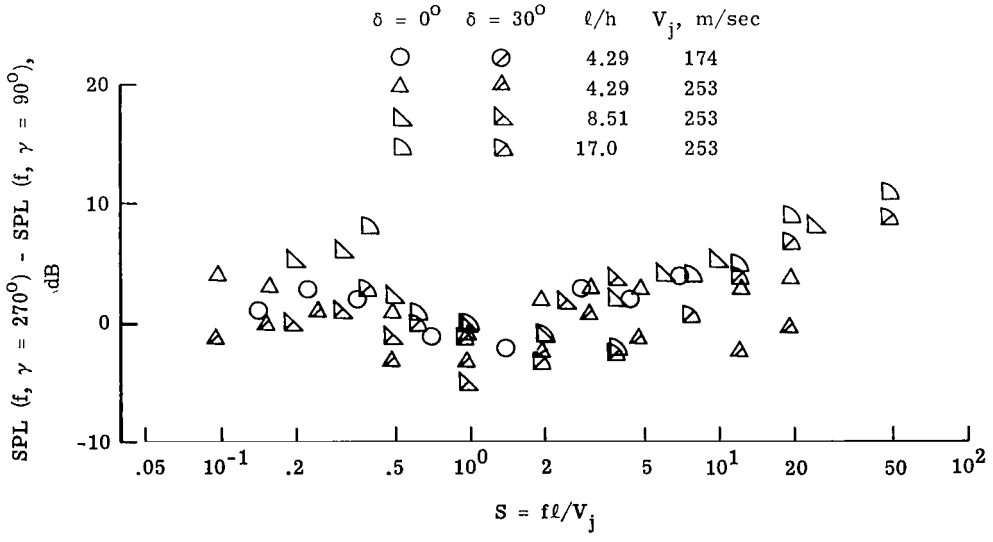

(b) w/h = 50.

Figure 15.- Effect of acoustic shielding on spectral data.

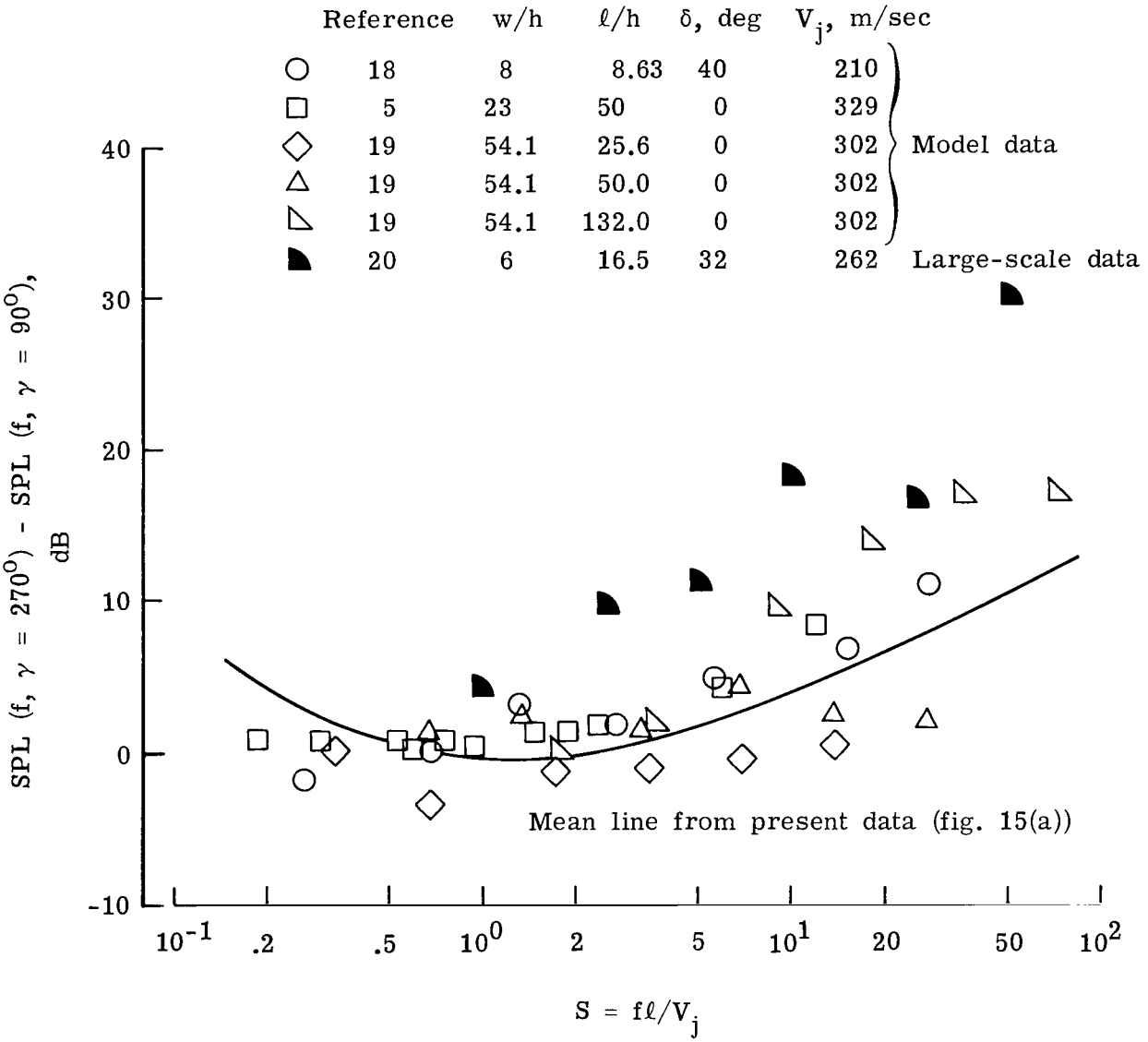

Figure 16.- Effects of acoustic shielding on spectral data as reported in references 5, 18, 19, and 20.

NATIONAL AERONAUTICS AND SPACE ADMINISTRATION
WASHINGTON, D.C. 20546

OFFICIAL BUSINESS
PENALTY FOR PRIVATE USE $300

SPECIAL FOURTH-CLASS RATE BOOK

POSTAGE AND FEES PAID
NATIONAL AERONAUTICS AND SPACE ADMINISTRATION
451

U.S.MAIL

209 001 C1 U H 770311 S00903DS
DEPT OF THE AIR FORCE
AF WEAPONS LABORATORY
ATTN: TECHNICAL LIBRARY (SUL)
KIRTLAND AFB NM 87117

If Undeliverable (Section 158 Postal Manual) Do Not Return

"The aeronautical and space activities of the United States shall be conducted so as to contribute . . . to the expansion of human knowledge of phenomena in the atmosphere and space. The Administration shall provide for the widest practicable and appropriate dissemination of information concerning its activities and the results thereof."

—NATIONAL AERONAUTICS AND SPACE ACT OF 1958

NASA SCIENTIFIC AND TECHNICAL PUBLICATIONS

TECHNICAL REPORTS: Scientific and technical information considered important, complete, and a lasting contribution to existing knowledge.

TECHNICAL NOTES: Information less broad in scope but nevertheless of importance as a contribution to existing knowledge.

TECHNICAL MEMORANDUMS: Information receiving limited distribution because of preliminary data, security classification, or other reasons. Also includes conference proceedings with either limited or unlimited distribution.

CONTRACTOR REPORTS: Scientific and technical information generated under a NASA contract or grant and considered an important contribution to existing knowledge.

TECHNICAL TRANSLATIONS: Information published in a foreign language considered to merit NASA distribution in English.

SPECIAL PUBLICATIONS: Information derived from or of value to NASA activities. Publications include final reports of major projects, monographs, data compilations, handbooks, sourcebooks, and special bibliographies.

TECHNOLOGY UTILIZATION PUBLICATIONS: Information on technology used by NASA that may be of particular interest in commercial and other non-aerospace applications. Publications include Tech Briefs, Technology Utilization Reports and Technology Surveys.

Details on the availability of these publications may be obtained from:

SCIENTIFIC AND TECHNICAL INFORMATION OFFICE

NATIONAL AERONAUTICS AND SPACE ADMINISTRATION

Washington, D.C. 20546